USCAP 2018

ABSTRACTS

PEDIATRIC PATHOLOGY
(1985-2010)

107TH ANNUAL MEETING
GEARED TO LEARN

MARCH 17-23, 2018

Vancouver Convention Centre
Vancouver, BC, Canada

PEDIATRIC PATHOLOGY

1985 Biomolecular changes associated with Preeclampsia by Fourier Transform Infrared (FT-IR) Spectroscopic Imaging

Oluwatobi Adelaja[1], *Vishal Varma*[2], *Andre Kajdacsy Balla*[3], *Michael J Walsh*[1]. [1]University of Illinois at Chicago, Chicago, IL, [2]UIC Hospital, Chicago, IL

Background: Recent evidence has implicated circulating angiogenic and antiangiogenic factors as the main mediators of the clinical symptoms of the maternal syndrome of preeclampsia. The placenta gross and microscopic examination is always used as confirmatory towards the clinical diagnosis of preeclampsia and cannot be used to exclude the diagnosis. However, in spite of the unique tissue biology of preeclampsia microscopic examination may not always yield diagnostic information. FT-IR is an imaging modality that allows for label-free imaging of tissue biochemistry to examine for biomolecular changes such as protein confirmation changes. Herein, we hypothesize that utilization of FT-IR spectroscopy will give a robust spectra of preeclampsia when compared to appropriate controls.

Design: We utilized a placenta tissue microarray (TMA) that consists of individual cores of the chorionic plate (P1), middle chorionic villi (P2), and basal plate (P3) for both preeclamptic (n = 38) and nonpreeclamptic tissue (n = 41). Samples with the clinical diagnosis of preeclampsia with chronic hypertension, preeclampsia with chronic hypertension and diabetes, preeclampsia with diabetes, and biological therapeutics were excluded from our analysis. Multivariate techniques such as principal component analysis and linear discrimination analysis were utilized to differentiate the two groups.

Results: Analysis of P1, P2, and P3 was performed independent of one another. We collected FT-IR data from the TMA and extracted biochemical signatures from the placenta tissue. P3 showed the best biochemical distinction between normal (n = 27) and preeclamptic (n = 19) placenta, with a misclassification rate of 7 out of 46 samples (Fig 1). P1 showed the poor biochemical distinction between normal (n = 33) and preeclamptic (n = 34) placenta, with a misclassification rate of 20 out of 67 samples (Fig 2A). P2 also demonstrated weak biochemical distinction between normal (n = 28) and preeclamptic (n = 22) placenta, with a misclassification rate of 15 out of 50 samples (Fig 2B).
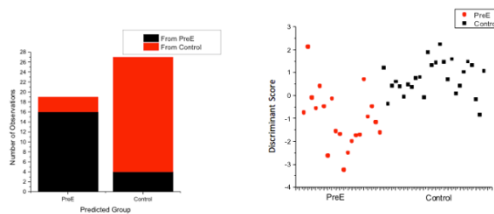

Figure 1. Number of observation per cohort for basal plate and PCA-LCA Analysis
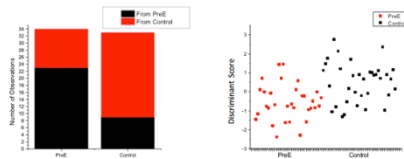

Figure 2A. Number of observation per cohort for chorionic plate and PCA-LCA Analysis
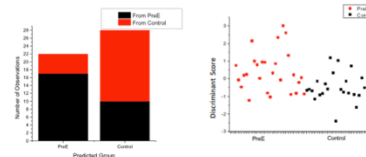

Figure 2B. Number of observation per cohort for middle chorionic villus and PCA-LCA Analysis

Conclusions: FT-IR is an emerging tool for biomarkers analysis of formalin-fixed paraffin-embedded tissue in a nondestructive manner. Our data suggest that the basal plate show the best biochemical distinction between preeclamptic versus nonpreeclamptic placenta. The tissue core from P3, which consists of both chorionic villi and decidualized endometrium, was the best predictor of preeclampsia. However, spectra changes cannot be reliably discern from both P1 and P2.

1986 Biliary Atresia: Have You Noticed Those Large Arterioles?

Fatimah Alruwaii[1], *Natalia Rush*[2], *Romil Saxena*[3]. [1]Indiana University School of Medicine, Indianapolis, IN, [2]Indianapolis, IN, [3]Indiana Univ/ Medicine, Indianapolis, IN

Background: Biliary atresia (BA) is characterized histologically by features that reflect severe biliary obstruction at the hilum. There is an intense ductular reaction comprised of proliferating bile ductules associated with neutrophils and portal fibrosis. The bile ductules appear dilated and may contain bile plugs. Although hepatic arterioles are not considered to be an integral part of this response, we (and others, anecdotally) have noticed that they appear prominent and thickened. In this context, it is pertinent that the hepatic artery represents the sole arterial supply to the biliary tract, which also explains the close anatomical proximity and perhaps, the nearly identical diameters of the two structures. We systematically studied the dimensions of paired hepatic arterioles and bile ducts, as well as the ratios of bile duct to hepatic artery diameters (BD:HA) in BA, and compared them to an age matched group of infants with neonatal hepatitis.

Design: The pathology database was queried to identify liver core and wedge biopsies performed on infants less than 12 weeks of age with BA (study group) and neonatal hepatitis (control group). Morphometric analysis was performed on 3 μ-thick sections from formalin fixed, paraffin embedded tissue utilizing a calibrated Nikon DS Camera Control Unit DS-L1 by a pathologist who was blinded to the diagnoses. Cross-sectional profiles of paired hepatic arterioles and bile ducts were identified on trichrome-stained slides. Tangential profiles of hepatic arteries and bile ducts, and non-paired hepatic arterioles and bile ducts were excluded. For each hepatic arteriole, the widest cross-sectional and luminal diameters were measured, and used to calculate the arteriolar wall thickness. The widest cross-sectional diameter of the accompanying bile duct was measured. The ratio of the cross-sectional diameters of the bile duct to hepatic artery (BD:HA) was calculated for each pair.

Results: Results are shown in Table 1.

Comparison of bile ducts and hepatic arterioles in biliary atresia to neonatal hepatitis			
	Biliary atresia (Fig.1)	**Neonatal hepatitis (Fig.2)**	**P value**
Age in weeks	2-12 (8.9)	3-12 (7.1)	0.121
Gender (M:F)	7:3	6:3	N/A
Bile duct - hepatic arteriole pairs (n)	29	21	N/A
Bile duct diameter in μm (mean)	34-99 (69)	24-57 (45)	0.0004
Arteriole cross sectional diameter in μm (mean)	40 -99 (68)	28-88 (59)	0.03156
Arteriole luminal diameter in μm (mean)	14-52 (30)	14-46 (28)	0.34722
Arteriole wall thickness in μm (mean)	8-34 (19)	4-29.5 (15)	0.089
Bile duct:hepatic arteriole ratio	058-1.57 (1.02)	0.5-1.0 (0.78)	0.01
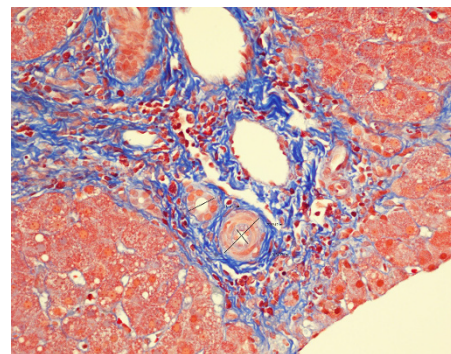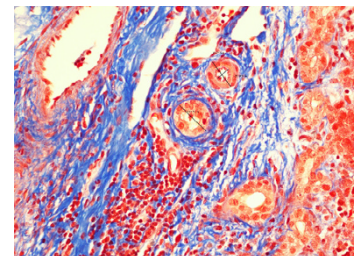
1. Compared to neonatal hepatitis,
   - hepatic arterioles are enlarged and thickened in BA, as evidenced by differences in their cross-sectional diameter (statistically significant) and wall thickness.
   - bile ducts are enlarged in BA, with a corresponding increase in the BD:HA ratio (both parameters, statistically significant).

2. Prominent and thickened hepatic arterioles may serve as an additional clue for the histological diagnosis of BA.

1987 Specificity of BCOR Immunohistochemistry in Pediatric Renal Neoplasia

Pedram Argani[1], Bruce Pawel[2], Sara Szabo[3], Miguel Reyes-Múgica[4], Cristina R Antonescu[5]. [1]Johns Hopkins Hospital, Ellicott City, MD, [2]The Children's Hospital of Philadelphia, Cherry Hill, NJ, [3]Cincinnati Children's Hospital Medical Center, Cincinnati, OH, [4]Children's Hospital of Pittsburgh of UPMC, Pittsburgh, PA, [5]Memorial Sloan Kettering Cancer Center, New York, NY

Background: Clear cell sarcoma of the kidney (CCSK) harbors internal tandem duplications in the last exon of the *BCOR* gene in over 90% of cases, with a smaller subset harboring *YWHAE-NUTM2B/E* or *BCOR-CCNB3* gene fusions. All of these genetic abnormalities result in a transcriptional signature characterized by high *BCOR* mRNA expression. Nuclear labeling for BCOR by immunohistochemistry (IHC) has been demonstrated to be a highly sensitive marker of CCSK (Am J Surg Pathol 2016; 40:1670-1678). The specificity of BCOR IHC in the context of pediatric renal neoplasia has not previously been studied.

Design: We evaluated whole sections from 62 neoplasms, including 32 Wilms tumors, 10 congenital mesoblastic nephromas (CMN) (1 classic, 5 cellular, 4 mixed), 8 CCSK, 8 metanephric stromal tumors (MST), 2 rhabdoid tumors of the kidney (RTK), 1 renal PNET and 1 sclerosing epithelioid fibrosarcoma (SEF). We performed immunohistochemistry for BCOR using clone C-10 (SC-514576; Santa Cruz, Dallas TX) generated against the N-terminus of BCOR at a dilution of 1:150 as done previously. Tumors were evaluated on the basis of intensity of labeling (strong, moderate, weak, or negative) and the percentage of positive neoplastic cells. Only nuclear labeling was counted. Neoplasms with less than 10% labeling were considered minimally positive, neoplasms with moderate to strong labeling in 10-50% of neoplastic cells were considered focally positive, while neoplasms with moderate to strong labeling in greater than 50% of cells were considered diffusely positive.

Results: BCOR IHC in Pediatric Renal Neoplasms

Tumor Type	Completely Negative	Minimally Positive	Focally Positive	Diffusely Positive
CCSK (n=8)	0	0	0	8 (100%)
Wilms (n=32)	13 (41%)	15 (47%)	4 (12%)	0
CMN (n=10)	5 (50%)	3 (30%)	2 (20%)	0
MST (n=8)	5 (63%)	3 (37%)	0	0
SEF (n=1)	0	0	1 (100%)	0
PNET (n=1)	1 (100%)	0	0	0

Conclusions: Diffuse nuclear IHC labeling for BCOR using previously published conditions is highly sensitive and specific for the diagnosis of CCSK in the setting of pediatric renal neoplasia. Nonetheless, caution is required (particularly in limited biopsy material) as other neoplasms may occasionally show focal labeling.

1988 Children with Refractory Respiratory Symptoms and Bronchial Ciliary Dysmotility have a High Prevalence of Structural Airway Anomalies and Lower Respiratory Infections

Helen Cathro[1], Andrea Garrod[2], W. Gerald Teague[3]. [1]UVA School of Medicine-Pathology, Charlottesville, VA, [2]University of Virginia, [3]University of Virginia, Charlottesville, VA

Background: Ciliary dysmotility is detrimental to mucociliary clearance and may cause significant respiratory morbidity and mortality. We examined the clinical features of children without inherited primary ciliary dyskinesia who had ciliary immobility (CI) on bronchoscopic specimens. The primary purpose of the study was to evaluate in cross-section the features of children with (CM) and without intact cilia.

Design: Children (n=211) with refractory wheezing or asthma underwent diagnostic bronchoscopy, bronchoalveolar lavage (BAL) and bronchial brushings. Fresh bronchial epithelial cells submitted in RPMI underwent ciliary motion evaluation using real time microscopy by a cytology fellow followed by a faculty cytopathologist.

Results: Eighteen children (8.5%) with CI were more likely to be pre-school age (p < 0.05). There were no differences by sex or race. Structural anomalies (laryngeal clefts and trachea- or broncho-malacia) occured in 61% vs. 36% of CI vs. CM respectively (p = 0.03). 30% of non-asthmatic children lacked motility compared to 6% of asthmatics (p = 0.001). Only 2 CM cases had ciliary ultrastructural examination; one had no abnormalities and the other had loss of inner dynein arms only. There was no difference in BAL granulocyte phenotype in CI and CM cases. There was a trend towards lower total blood eosinophilia, but no difference in atopy in the two groups. There was a significant difference in viral detection (59% and 32% in CI and CM cases respectively, p=0.02). 44% of CI cases had positive rhinovirus transcripts versus 27% of CM (p>0.05). 19% of CM were positive for non-enteroviruses versus 4% of CI (p = 0.01). An unpaired t-test comparing outcomes in the 2 groups showed significant differences: CI children were on average 4 years younger, had lower total IgE, and fewer BAL eosinophils (p < 0.05 for all).

Conclusions: 8.5% of children who undergo bronchoscopy for refractory respiratory symptoms lack ciliary motility. These children are younger, have an almost 2-fold higher prevalence of structural anomalies, less asthma and less allergen sensitization, but a strikingly higher prevalence of lower respiratory tract viral infections, primarily non-enteroviruses. Ciliary motility studies in this group of patients with likely acquired/transient airway malacia can help guide treatment. This study serves as a reminder that while ciliary motility studies are not specific for inherited primary ciliary dysplasia, they can provide useful clinical information in other patients.

1989 Molecular Profiling of Embryonal (Undifferentiated) Sarcoma of the Liver

Ladan Fazlollahi[1], Susan Hsiao[2], Amy Coffey[3], Mahesh Mansukhani[1], Darrell J Yamashiro[1], Helen Remotti[4]. [1]Columbia University Medical Center, New York, NY, [2]Flushing, NY, [3]Dell Children's Hospital, [4]Dobbs Ferry, NY

Background: Embryonal (undifferentiated) sarcoma of the liver (ES) is a rare, aggressive pediatric malignancy. The immunohistochemical profile of these tumors is often nonspecific with a variable staining profile. The molecular profile of these tumors is not well-characterized. The aim of this study is to expand and better define the molecular profile of these tumors.

Design: Following IRB approval, four cases of ES in the pediatric age group (0 to 18 years) were identified in our intradepartmental cross-files within the last 20 years. Columbia Combined Cancer Panel (CCCP), a targeted exome sequencing assay, with copy number variant analysis (CNVA) was performed on the archival formalin-fixed paraffin-embedded tissue of tumor/normal pairs in all four cases.

Results: Two of four cases showed different TP53 mutations, while one case showed PIK3C2G mutation, and no mutation was found in the fourth case. Our cases showed amplifications and deletions of variable genes, as listed in Table 1.

CCCP with copy number variant (CNV) analysis of cases

Case	Age (y)/ Gender	CCCP	CNV
1	5 y/ male	TP53 mutation, R273H missense	PIK3CA (amplification) FGFR4 (deletion) PTEN (deletion) TP53 (deletion) NF2 (deletion) TERT (deletion)
2	4 y/ male	-	AKT3 (amplification) MDM2 (amplification)
3	5 y/ male	TP53 mutation, R175H missense	PDGFRA (amplification) EGFR (amplification)
4	7 y/ male	PIK3C2G mutation, K122Q missense	FGFR1 (amplification) ERBB3 (amplification) CDK4 (amplification) CDKN2A (deletion)

Conclusions: We did not identify a characteristic genetic alteration or a clinically targetable gene mutation in our analysis.

1990 Perineural Invasion in Ewing Sarcoma - a Novel Mechanism of Tumor Dissemination in a Mouse Xenograft Model

Susana Galli[1], Sung-Hyeok Hong[2], Mina Adnani[3], Ewa Izycka-Swieszewska[4], Joanna Kitlinska[3]. [1]Rockville, MD, [2]Georgetown University Medical Center, Washington, DC, [3]Georgetown University Medical Center, [4]Medical University of Gdansk, Poland

Tumor dissemination and relapse are the major problems in Ewing sarcoma (ES) treatment. Yet, the mechanisms driving these processes are unknown.

To elucidate the routes of ES metastatic spread, we used an orthotopic xenograft model. Three different ES cells lines (TC-32, TC-71 and SKES) were injected into the gastrocnemius muscles of SCID/beige mice. Once the primary tumors reached the desired volume, they were excised by limb amputation. Subsequently, tumor dissemination was monitored by MRI and confirmed by histopathological analyses.

Aside from typical hematogenous metastases, such as bone and lung lesions, we have also observed frequent perineural tumor dissemination manifested by the presence of migratory ES cells along the nerves adjacent to the primary tumors. This phenomenon was associated with formation of recurrent tumors at the amputation sites, as well as paravertebral tumors at lumbo-sacral, thoracic and cervical levels. These tumors showed perineural and sympathetic ganglion compromise. Interestingly, the level of perineural invasion (PNI) was dependent on the expression of neuropeptide Y (NPY) in ES cells. NPY is a neuronal protein released from peripheral sympathetic neurons, but also highly expressed in ES cells along with its receptors. The xenografts derived from ES cell lines not releasing endogenous NPY (TC71, TC32) exhibited frequent PNI in tumor-bearing limbs, as well as a high number of recurrent tumors in the surgery site and paravertebral tumors (70% and 100% of mice with evidence of PNI for TC71 and TC32 xenografts, respectively). These processes were less common in ES xenografts derived from NPY-rich SK-ES cells (35% of mice with signs of PNI). In line with these observations, NPY knock-down in SK-ES xenografts drastically accelerated formation of spinal tumors (60% of mice). Notably, in 40% of mice bearing SK-ES NPY shRNA xenografts the paravertebral tumors developed before the primary tumor growth was detectable at the site of ES cell injection.

Altogether, our data indicate that lack of endogenous peptide in ES cells expressing high levels of its receptors triggers chemotactic effects of NPY released from neighboring peripheral nerves, facilitating PNI. Further studies are required to determine which of NPY receptors is responsible for its chemotactic properties. Blocking pathways responsible for PNI in ES, e.g. NPY receptors, may lead to development of novel therapies preventing disease dissemination and recurrence.

1991 Inherited Bone Marrow Failure Syndromes and Risk for Development of Myeloid Neoplasms: Report of 3 Cases

Maria Isales[1], Alicia Lenzen[2], Rachel Mariani, Joanna Weinstein[2], Shunyou Gong. [1]Chicago, IL, [2]Northwestern Memorial Hospital

Background: The inherited bone marrow failure syndromes (IBMFS), consisting of over 25 disease entities that classically present with cytopenias, have been associated with an increased risk of secondary malignancies, particularly myelodysplastic syndrome (MDS) and acute myeloid leukemia (AML). Although the 2016 World Health Organization Classification of Tumors of Hematopoietic and Lymphoid Tissues (WHO) is introducing a new provisional entity "myeloid neoplasms with germline predisposition", which covers these IBMFS to some extent, the association of IBMFS with myeloid neoplasms has not been well studied, due to rare cases and under-recognition of underlying marrow failure before MDS/AML develops.

Design: A retrospective chart review of pediatric (0-21 years of age) patient records from 2012-2017 at our institution was performed. Patients were identified based on clinical diagnoses of Schwachman Diamond Syndrome, Fanconi anemia, thrombocytopenia absent radii syndrome (TAR), Diamond-Blackfan anemia, and dyskeratosis congenita. Pathology reports, flow cytometric studies, cytogenetics, and clinical data were reviewed.

Results: Fifty-two patients with a presumptive diagnosis of IBMFS were identified with 3/52 (6%) patients progressing to MDS/AML. An initial diagnosis of MDS/AML was made at ages 8, 11, and 18 for patients 1-3, respectively. The three patients met the current WHO diagnostic criteria for a myeloid neoplasm with germ line predisposition. The presenting symptoms included fever, pancytopenia, and weight loss. The blast percentage in the bone marrow core biopsy for cases 1 and 2 ranged from 10-15% while the blast percentage in case 3 was 15-20%. The bone marrow from case 1 demonstrated biallelic mutations in the FANCA gene, case 2 demonstrated a 600 base pair microdeletion at chr.1q21.1, including RBM8A gene, and case 3 demonstrated double heterozygosity in two pathogenic mutations of the SDS gene. Follow-up ranged from 1 month to 11 years.
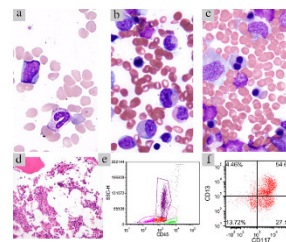
Figure 1: TAR syndrome patient
a. Peripheral blood
b. Aspirate 1
c. Aspirate 2
d. Core H&E
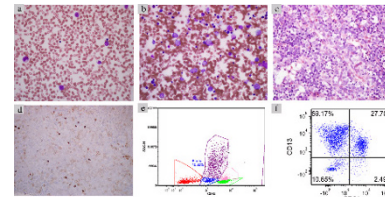e. Flow cytometry 1
f. Flow cytometry 2

Figure 2: SDS patient
a. Peripheral blood
b. Aspirate
c. Core H&E
d. CD117 immunostain
e. Flow 1
f. Flow 2

Conclusions: We report three cases of MDS/AML progressed from IBMFS and aim to draw attention to the underdiagnosis of IBMFS due to the variability in phenotypic presentations and undiscovered mutations. Our data shows that bone marrow failure syndromes may be diagnosed following an initial diagnosis of MDS/AML as seen in our SDS case. Particularly, TAR syndrome is not usually considered to be associated with progression to MDS/AML. A timely and accurate diagnosis with subsequent genetic counseling and management is critical.

1992 Pediatric Membranous glomerulonephritis (MGN): A Multi-institutional Study of Phospholipase A2 Receptor Expression in Primary versus Secondary MGN

DongHyang Kwon[1], Bakri Alzarka[2], Kyungmin Ko[1], Bhaskar Kallakury[3], Asha Moudgil[2]. [1]MedStar Georgetown University Hospital, Washington, DC, [2]Children's National Medical Center, [3]Georgetown Univ Hosp, Washington, DC

Background: Autoimmunity against M2-type Phospholipase A2 receptor (PLA2R) is implicated in the pathogenesis of primary MGN in adults. Since the discovery, immunohistochemistry (IHC) has been increasingly employed in the diagnosis of primary MGN by detecting PLA2R antigens in glomerular subepithelial deposits. However, the status of PLA2R in pediatric MGN, a relatively rare disorder, is not well established. In this study, we present a multi-institutional experience of PLA2R expression in primary versus secondary MGN in a pediatric population.

Design: 36 pediatric renal cases (age ≤19 years) with diagnosis of MGN were retrospectively collected from two different institutions (Georgetown University Hospital and Children's National Medical Center, Washington DC).IHC was performed on tissue sections using PLA2R monoclonal antibody (CL0474, 1:1500 dilution) and IgG4 monoclonal antibody (HP6025, 1:500 dilution). PLA2R and IgG4 results were scored blindly, then compared with clinical, morphologic, immunofluorescence (IF) and electron microscopy (EM) findings in primary and secondary MGN.

Results: Out of 36 cases of MGN, 3 met the criteria of primary MGN (without any known etiology). Out of 33 secondary MGN, 27 cases were lupus nephritis (*bona fide* secondary MGN) and the remaining 6 cases were clinically classified as secondary MGN due to concurrent non-lupus medical conditions. PLA2R was positive (glomerular basement membrane staining) in all 3 primary cases (100%, Fisher's exact test, p < 0.03), 5 of 6 non-lupus secondary MGN (83%, Fisher's exact test, p <0.01), and 4 of 27 (15%) lupus secondary MGN (see diagram 1). On comparison with morphologic, IF and EM findings, all five PLA2R+ non-lupus secondary MGN showed features resembling primary rather than secondary MGN without a "full-house IF pattern" and deposits confined to subepithelium on EM (see table 1). IgG4 was negative in all pediatric MGN.

Table 1: Morphologic features of the four PLA2R positive non-lupus membranous GN cases resembling primary rather than secondary MGN.

MGN status	Etiology	Other H&E Findings*	TRS	IF findings	EM Deposit location
Secondary	IPEX syndrome	MP	Yes	Negative	Subepithelial
Secondary	IPEX syndrome	MP	Yes	Negative	Subepithelial
Secondary	Mixed connective tissue disease	NONE	Yes	IgG	Subepithelial
Secondary	Ganglioneu-roblastoma	NONE	No	No glomerus	Subepthelial
Secondary	Evans syndrome	MP	Yes	IgG and C3	Subepthelial

*MP: mesangial proliferation;

Diagram 1
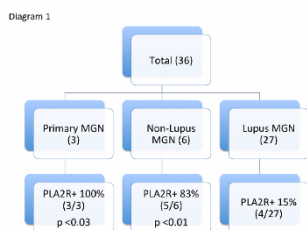
Conclusions: While the PLA2R staining results in primary and lupus secondary MGN are consistent with reported literature in adult patients, the high percentage of PLA2R positivity in non-lupus secondary MGN raises questions that need to be further explored with regard to whether these cases involve two separate medical conditions of unrelated etiology or if the underlying medical conditions truly lead to autoimmunity against PLA2R antigen. Clinically, PLA2R positivity in a child should prompt testing for other autoimmune or malignancy before labelling it as primary MGN.

1993   Clinicopathological Study of 79 Cases of Infantile Leukemia: Where Should the Line for Congenital Leukemia be Drawn for Practical Purposes?

Xin Liu[1], *Catherine Luedke*[2], *Lianhe Yang*[3], *Chuanyi M Lu*[4], *Rachel Jug*[5], *Zenggang Pan*[6], *Dehua Wang*[7], *Robert Lorsbach*[8], *Yang Shi*[9], *Virginia Knez*[10], *Xiayuan Liang*[11], *Endi Wang*[12]. [1]Duke University Medical Center, Cary, NC, [2]Duke University Medical Center, Durham, NC, [3]Duke Health, [4]UC San Francisco, San Francisco, CA, [5]Duke Health, Durham, NC, [6]Aurora, CO, [7]Cincinnati Children's Hospital Medical Center, Blue Ash, OH, [8]Cincinnati Children's Hospital, Cincinnati, OH, [9]Montefiore Medical Center, [10]University of Colorado School of Medicine, Aurora, CO, [11]Children's Hospital Colorado, Aurora, CO, [12]Duke University Medical Center

Background: Congenital leukemia (CL), defined as leukemia occurring in a neonate, is a specific category within infantile leukemias. The clinicopathologic features for infantile leukemias other than CL seem to vary with a significant fraction resembling CL.

Design: With institutional approval, 79 cases of infantile leukemia were retrieved from our pathology database, and their clinicopathological findings were retrospectively evaluated.

Results: Of 79 cases, 36 were male, and 43 were female patients. 93.3% of the patients were born full term with birth weight ranging from 2.6 to 3.5 kg (median=3.1 kg), while 6.7% wereborn prematurely (median 34 weeks) with median birth weight of 3.5 kg. Patients presented with symptoms of leukemia at ages ranging from the first day of birth to 16 months, with median age of 5 months. 8 cases were diagnosed within 30 days of birth, consistent with CL. The majority of patients presented with signs and symptoms including skin bruising, leukocytosis, anemia/thrombocytopenia, and/or splenomegaly. Types of leukemia included B-lymphoblastic leukemia (B-ALL) in 50 (63%) cases, acute myeloid leukemia (AML) in 24 (30%) cases, T-lymphoblastic leukemia (T-ALL) in 3 (4%) cases, and other myeloid neoplasms in 2 (3%) cases. Cytogenetic studies revealed clonal abnormalities in 71 (92%) cases, including MLL (11q23) gene rearrangement in 47 (66%), hyperdiploidy in 8 (11%), and other abnormalities in 16 (23%) cases. Interestingly, among B-ALL patients, when plotting against age, the MLL gene rearrangement inversely correlated with age (months), with abrupt decline at 8 months (Figure 1). Most of the patients received treatments corresponding to leukemia type. Out of 79 patients, with median follow up of 24 months, 57% died of disease progression, with average overall survival of 95 ± 13 months. When stratified by age, the group of ≤8 months had an average overall survival (49 ± 9 months) which was significantly shorter than the group of ≥8 months (131 ± 21 months; $P < 0.05$) (Figure 2).
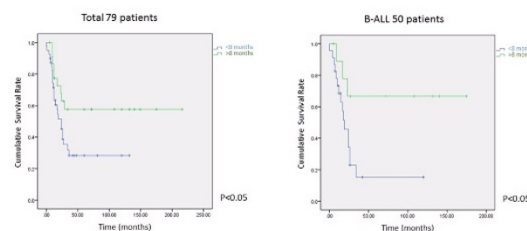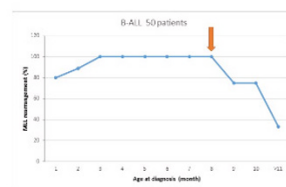
Conclusions: Infantile leukemia demonstrates a unique cytogenetic profile, featuring a high fraction of MLL gene rearrangements, particularly those occurring within 8 months of life. The clinical outcome of infantile leukemia is also extremely poor despite vigorous treatment. CL, as a special subcategory of this disease, has even more dismal outcomes, and the biological behavior remains similar with age until 8 months. Additional large cohort studies are needed to further classify this disease entity.

1994   Comparison of DUX4 Immunohistochemical Expression in CIC-Rearranged Sarcomas and Other Primitive Sarcomas

Kara A Lombardo[1], *Gino R Somers*[2], *Shaolei Lu*[3], *Mary Shago*[2], *Sonja Chen*[4], *Evgeny Yakirevich*[1], *Shamlal Mangray*[1]. [1]Rhode Island Hospital, Providence, RI, [2]The Hospital for Sick Children, Toronto, ON, Canada, [3]Brown University, Providence, RI, [4]Rhode Island Hospital, Providence, RI

Background: A subset of primitive sarcomas (PrSs) with round cell and/or spindle cell morphology resembling Ewing sarcoma/ primitive neuroectodermal tumors (EWS/PNETs) but lacking the characteristic *EWSR1* rearrangement have been found to harbor rearrangement of the *CIC* gene. These *CIC*-rearranged (*CIC*+) sarcomas are the most common form of *EWSR1* negative Ewing-like sarcomas and fusion with the *DUX4* gene occur in the vast majority of cases. Recently immunohistochemical (IHC) expression of DUX4 using a commercially available monoclonal antibody (Mab) to the C-terminus of the human DUX4 protein (clone P4H2) was reported to be highly sensitive (100%) and specific (100%) in 5 *CIC-DUX4* cases compared to 76 other small round cell tumors.

Design: Archival cases of *CIC*+ sarcomas (8 genomically proven *CIC-DUX4*+, and 1 *CIC*+ by FISH), EWS/PNETs (17), *BCOR-CCNB3* sarcomas (2), desmoplastic small round cell tumors (DSRCTs; 12), rhabdomyosarcomas (RMS; 19), and synovial sarcomas (SS;10) fulfilling IHC and molecular criteria were included in this study. DUX4 IHC staining with the same Mab at a dilution of 1:200 was performed on whole sections of biopsies or resections with a minimum of one thousand neoplastic cells available for scoring with appropriate positive and negative controls. Semiquantitive scoring of IHC staining was based on intensity and extent of nuclear staining: 0, 0% of cells positive; 1+, weak staining or <10% of cells positive; 2+,10-50% of cells moderately to strongly positive, and 3+, >50% of cells moderately or strongly positive. A score of 2+ or 3+ was considered positive.

Results: DUX4 IHC expression in this study is summarized in the Table. The 6 *CIC*+ sarcomas that were DUX4+ included a FISH+ needle biopsy case (strong, >75%), and 5 of the *CIC-DUX4*+ cases (1 case with 40-50% moderate, 1 case with 50-75% moderate, 1 case with >75% moderate and 2 cases with > 75% strong staining). The other positive PrSs were 1 *BCOR-CCNB3* tumor (40-50%, moderate), 1 EWS/ PNET (10-20%, moderate) and 1 DSRCT (20-25%, moderate). Overall the sensitivity was 66.7%, specificity was 95%, positive predictive value was 66.7% and negative predictive value was 95%.

Table. DUX4 expression in *CIC*-rearranged and other primitive sarcomas.

Sarcomas	DUX4 Immunohistochemical Score				Overall Positive Staining (%)
	0	1+	2+	3+	
CIC+ (n=9)	1	2	1	5	66.7
EWS/PNETs (n=17)	16	0	1	0	5.88
BCOR-CCNB3+ (n=2)	0	1	1	0	50.0
DSRCTs (n=12)	9	2	1	0	8.33
RMSs (n=19)	19	0	0	0	0
SSs (n=10)	10	0	0	0	0

Conclusions: In this larger series of *CIC*+ sarcomas (9 vs 5 cases), the sensitivity and specificity of DUX4 IHC expression was lower than that previously reported. Further studies are required to assess the potential application of the DUX4 Mab for clinical practice.

1995 Use of K36M Mutant Histone H3 Immunohistochemistry in the Diagnosis of Pediatric Chondroblastoma

Chelsea Maedler[1], *Fang Bu*[1], *Fusheng Yang*[1], *David Parham*[1]. [1]Children's Hospital Los Angeles, Los Angeles, CA

Background: Chondroblastoma is a benign cartilaginous lesion that typically presents in childhood and shows histologic overlap with other benign and malignant bone tumors. Diagnostic immunohistochemistry (IHC) for chondroblastoma has previously been limited to S100, a nonspecific stain. The H3 K36M mutated oncohistone has been described as a more specific marker of chondroblastoma and giant cell tumors and is part of a family of altered histones that define the molecular signatures in various pediatric malignancies including glioblastomas. An IHC antibody directed against the H3K36M mutation may assist in the diagnosis of these lesions.

Design: A total of 108 cases including 57 chondroblastomas, 4 chondromyxoid fibromas, 17 chondrosarcomas, 10 giant cell tumors of bone (GCT), 10 osteosarcomas and 10 aneurysmal bone cysts (ABC) were selected from our pathology archives. Anonymized data including patient age, gender, lesion location, final diagnosis, and decalcification were recorded. Tissue sections from all cases underwent IHC staining for anti-Histone H3K36M mutant protein (Millipore, Temecula CA). Immunoreactivity was graded as 4 (strong) if over 50% of cells exhibited nuclear staining, 3 (moderate) if 10-49% of cells showed staining, 2 (weak or focal) if staining was faint or present in less than 10% of cells, 1 if staining was barely perceptible but present at 10x, and 0 if staining was not visible above background.

Results: A summary of the IHC results is presented in Table 1. The commercially available H3K36M mutant antibody produced readily interpretable nuclear immunoreactivity in positive cases, although the intensity varied. Some background cytoplasmic staining was present in both chondroblastoma and other bone tumors. Using our scoring system, H3K36M mutant staining was minimal or absent in the other malignant and benign bone tumors examined. Moreover, H3K36M mutant was highly sensitive (95%) and specific (94%) for chondroblastoma and displayed a strong positive predictive value (95%) and negative predictive value (94%).

Table 1. IHC Results for Selected Cases

Final Diagnosis	n (no. subjected to decalcification)	No. Positive (Avg. Staining Score)	% Positive
Chondroblastoma	57 (43)	54 (2.8)	97
Chondrosarcoma	17 (13)	2 (1)	12
GCT	10 (3)	1 (3)	10
ABC	10 (5)	0 (0)	0
Osteosarcoma	10 (7)	0 (0)	0
Chondromyxoid Fibroma	4 (0)	0 (0)	0

Conclusions: Chondroblastoma is challenging to diagnose by histology alone, as it resembles both benign and malignant entities. The results of this study confirm that H3K36M mutant IHC is sensitive and specific for chondroblastoma and may be useful in the clinical diagnosis of this lesion.

1996 A Novel Biomarker For Prediction of Seizure-Free Outcome In Children And Adolescents With Focal Cortical Dysplasia Type II

Lili Miles[1], *Hansel Greiner*[2], *Francesco Mangano*[2], *Paul Horn*[2], *Michael Miles*[3]. [1]Nemours Children's Hospital, Orlando, FL, [2]Cincinnati Children's Hospital Med Ctr, [3]University of Central Florida College of Medicine, Orlando, FL

Background: The PI3K/Akt/mTOR pathway is important in pathogenesis of brain overgrowth disorders, including focal cortical dysplasia (FCD) associated with intractable epilepsy. In most FCD Type II (FCDII) cases hypertrophic neurons exhibit increased PI3K/Akt/mTOR signaling. Recently Akt was found to be a key determinant of brain overgrowth in a rodent model (*Neuroscience* 2017;354:196-207). Because an independent biomarker for prediction of seizure-free outcome in FCDII epilepsy patients has not been validated previously, we propose to evaluate Akt overexpression, using a novel immunohistochemical (IHC) technique, as a biomarker for predicting seizure-free outcome in children with pathology-confirmed FCDII.

Design: This retrospective study reviewed patients who had epilepsy surgery from 2008-2012. Institutional Review Board approval was obtained. Inclusion criteria were: age <18y, pathology-confirmed FCDIIa or FCDIIb, and follow-up evaluation (≥1y post surgery). Exclusion criteria were: FCD Types I or III, dual pathology, and hemispherectomy. IHC methods, published previously in *JNEN* 2013;79:884-891, determined the highest density/high power field (hpf,×40) of Akt1-positive neurons in resected cortical tissue. Receiver operator characteristic (ROC) analysis evaluated the validity of Akt1-positive neuron count for prediction of seizure-free outcome (ILAE classification 1). The IHC cutoff was selected using the highest Youden index (Sensitivity+Specificity-1).

Results: A total of 25 patients with FCDII were identified, including 8 FCDIIa and 5 FCDIIb, who were seizure-free, and 12 who were not seizure-free. Clinical characteristics were similar for seizure-free and non-seizure-free groups (Table 1). The Akt1-positive neuron count was significantly increased in the seizure-free study group (Table 1). ROC curve analysis had the highest predictive probability for seizure-free outcome at ≥7 Akt1-positive neurons/hpf. At that cutoff the following results were obtained: sensitivity=0.769, specificity=0.750, PPV=0.769, NPV=0.750, accuracy=0.760, and area-under-the-ROC curve=0.756 (P=0.007). The predicted probability graph (Figure 1) and ROC curve model (Figure 2) are shown for seizure-free (N=13) vs.non-seizure free (N=12) outcomes in 25 pediatric patients with FCDII.

Univariate analysis of post-operative variables comparing characteristics of seizure-free (SF) and non-seizure-free (NSF) outcome groups of 25 pediatric patients with pathology-confirmed FCD Type II. Mean (SD).

	SF N=13	NSF N=12	p-value
Gender (F)	6(46%)	3(25%)	0.41[a]
FCDIIa/FCDIIb	8/5	12/0	0.04[a]
Age at Epilepsy Onset (y)	3.8(4.9)	5.4(4.1)	0.26[b]
Age at Surgery (y)	9.1(5.4)	12.7(3.9)	0.10[b]
Duration of Epilepsy (y)	5.3(4.3)	7.3(3.6)	0.18[b]
Time to Follow-up (y)	1.3(0.5)	1.6(0.6)	0.17[b]
Number of Akt1-positive neurons/hpf	11.1(6.8)	6.1(5.8)	0.04[b]

FCD, focal cortical dysplasia; hpf, high power field (×40).
[a]Fisher exact test.
[b]Mann-Whitney test.

ROC Curve for Model
Area Under the Curve = 0.7564
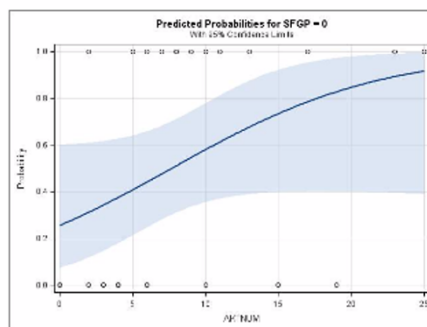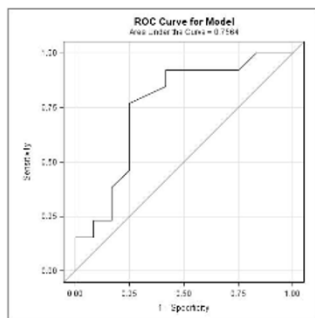
Conclusions: A novel IHC biomarker for increased Akt expression in cortical resections from pediatric FCDII patients predicts seizure-free outcome at a cutoff ≥7.0 Akt1-positive neurons/hpf, and should be further evaluated in a larger population.

1997 Lymphocytic Esophagitis in Children: A Condition in Search of a Disease

Tejal Patel[1], *Debbie Walley*[2], *Anas Bernieh*[3], *Ali Saad*[2]. [1]University of Mississippi Medical Center, Madison, MS, [2]University of Mississippi Medical Center, Jackson, MS, [3]University of Mississippi Med Ctr, Jackson, MS

Background: The significance of lymphocytic esophagitis (LyE) in children is poorly defined. Here we report the largest series of LyE in children with detailed description of the clinical and follow up findings.

Design: All esophageal biopsies performed on children (≤18 years-old) from January 2005 to May 2015 were reviewed. Only cases with ≥20 lymphocytes/high-power field and rare eosinophils (≤2) are included. Demographics, endoscopic findings and follow-up are retrieved from pathology reports and medical records in accordance with the institutional research board guidelines. Immunohistochemistry for CD3, CD20, CD4 and CD8 was performed. Lymphocytic count was generated by counting the numbers of lymphocytes at 40X in a single hot spot.

Results: Twenty-four patients fulfilled the search criteria (age range: 1-17.5 years; mean: 6.9 years). They consisted of 11 males (age range: 1-17.5; mean: 6.9 years) and 13 females (age range: 2-16.5 years; mean: 6.9 years). The most common presentation was dysphagia (33.3%) followed by reflux (29.2%), abdominal pain (29.2%), and nausea and vomiting (8.3%). Esophageal endoscopic findings ranged from normal to erosive esophagitis. Ileal and colonic endoscopy ranged from normal to severe active inflammation.

The mean number of lymphocytes was 40.4 (range 21-71 lymphocytes). There was correlation between the number of lymphocytes and a particular final diagnosis. In addition, there was no difference in the number of lymphocytes between males and females. The vast majority of lymphocytes expressed CD3 and, to a lesser degree, CD8. A minority expressed CD4 and CD20. There was no correlation between the immunophenotype and a particular diagnosis.

Follow-up showed that 7 patients were diagnosed with gastroesophageal reflux disorder, 7 patients with eosinophilic esophagitis, 3 patients with Crohn's disease, 1 patient with celiac disease, 1 patient with ulcerative colitis, and 3 patients with gastritis. Follow-up in 3 patients did not disclose any particular entity and, therefore, these patients were diagnosed with LyE.

Conclusions: Lymphocytes esophagitis in children remains a poorly defined entity. Our study suggests that a particular diagnosis is often not apparent at the onset of LyE and, therefore, a regular follow-up is required in order to identify the underlying disease. Our results also show that LyE is not associated with a particular disease but rather it represents a prelude to other better defined entities.

1998 Genomic Landscape of Pediatric Hepatocellular Carcinoma

Torsten Pietsch[1], *Alexandra Carmichael*[2], *Verena Dreschmann*[2], *Ivo Leuschner*[2], *Christian Vokuhl*[2]. [1]University of Bonn, Bonn, NRW, [2]University of Kiel

Background: Hepatocellular carcinomas (HCC) of childhood are rare neoplams. Their pathogenesis is believed to be different from HCC in adulthood. The differential diagnosis from hepatoblastoma (HBL) is important because of worse prognosis of pediatric HCC (pHCC) and different treatment approaches. However, the diagnosis by conventional histological analysis may be difficult in some cases. Informations on chromosomal alterations in pHCC are lacking. The aim of this study was to identify recurrent chromosomal aberrations, mRNA expression and epigenetic signatures in a larger cohort of pHCC and compare it to HBL to identify characteristic genomic alterations of pHCC.

Design: Genomic DNA was extracted from FFPE and fresh frozen samples of a cohort of 44 pHCC including 4 cases of the fibrolamellar subtype and 3 cases with partial fibrolamellar differentiation from the archives of the German Pediatric Tumor Registry, University of Kiel. Genome-wide copy analysis was performed by molecular inversion profiling. GISTIC analysis was done to identify significant large and focal aberrations. Epigenetic signatures were studies using methylation arrays, mRNA expression analyzed using HTA2.0 expression arrays. Protein expression and recurrent copy number alterations were validated using tissue microarrays.

Results: Most frequent copy number alterations were gains of chromosome 1q (68%), 2q (34%), 20 (34%), 6p (30%),19q (27%) and 8q (27%) and losses of chromosomal regions 1p (52%) and 4q (41%). In addition, GISTIC analysis identified several significant fokal alterations including losses of the *AXIN1* tumor suppressor locus on 15q26 in 41% of cases. 6/34 pHCC lacked any larger chromosomal imbalances. Of note, 5 of these 6 genomically stable tumors showed fibrolamellar differentiation. When pHCC were compared to HBL, both entities shared similar alterations including gains if 1q, 2, 8 and 20, but losses of 1p and 4q and gains of 19q were significantly more frequent in pHCC. Cluster analysis of expression and methylation data did not separate a specific pHCC cluster from HBL. Gene set enrichment analysis identified WNT signalling and ribosome profiles to be enriched in pHCC when compared to fetal fetal liver.

Conclusions: This genome-wide copy number, epigenetic and mRNA expression analysis of pHCC uncovered characteristic alterations and signatures which showed similarities to HBL but also indicated a specific pathogenesis of pHCC. Specific genetic alterations may help in the differential diagnosis of these tumors.

1999 A cohort of children with clinically suspected hypoxic ischemic injury: correlations to placental pathology, clinical outcome, and neonatal imaging findings

Wesley Samore[1], *Paul Caruso*[2], *Kalpathy Krishnamoorthy*, *Sara Bates*[2], *Drucilla Roberts*[2]. [1]Boston, MA, [2]Massachusetts General Hospital, Boston, MA

Background: Hypoxic-ischemic encephalopathy (HIE) is a critical cause of neurological morbidity in children. Placental pathology and neonatal brain imaging findings have not been well correlated to clinical outcomes in the setting of HIE.

Design: A cohort of 37 infants with clinically suspected hypoxic ischemic injury at birth was identified. Infants with evidence of cerebrovascular infarction by imaging or clinical examination were excluded from the study. Placentas from all cases were examined for pathology. Fetal vascular malperfusion (FVM) was diagnosed and graded based on the Amsterdam Placental Workshop Group Consensus Statement.

Results: Clinical data was available for 34 children, with a mean followup time of 3.75 years for non-deceased patients. 14 infants (38%) underwent therapeutic hypothermia for hypoxic ischemic encephalopathy (HIE). Autopsy data was available in 5 of the 6 deaths. Clinical outcomes included severe developmental delay or cerebral palsy in 6 children (17%), death in 6 children (17%), mild motor and/or sensory delays in 12 children (35%), and no significant abnormality in 7 children (20%), mild behavior issues in 2 children (6%), and seizures as the only sequelae in 1 child (3%). Rates of high grade FVM were significantly increased with severe developmental delay or cerebral palsy when compared with the normal outcome group (P = 0.0133). High grade FVM was present in 4 of 6 children with severe developmental delays or cerebral palsy, 3 of 12 children with mild motor and/or sensory delays, and none of the 7 children with normal outcome. Low grade FVM was not associated with clinical outcome and was present in one child with mild developmental delay and one normal child. Rates of central-type hypoxic ischemic injury on imaging (i.e. injury preferentially focused in the deep gray matter) were significantly increased in children with severe developmental delays or cerebral palsy (3 of 6 children) compared with rates in children with mild outcomes (1 of 12 children) (P = 0.0380). The proportion of placentas under the 10th percentile for gestational age was not statically different across the various clinical outcome groups.

Conclusions: In summary, imaging findings and placental pathology were collected in a cohort of children with suspected hypoxic ischemic injury and correlated to clinical outcomes. We found that high grade FVM was associated with increased neurological morbidity.

2000 DNA Methylation Analysis Defines Two Distinct Subgroups of Clear Cell Sarcoma of the Kidney

Teresa Santiago[1], *Michael Clay*[1], *Sariah Allen*[1], *Cynthia Cline*[1], *Brent Orr*[1]. [1]St Jude Children's Research Hospital, Memphis, TN

Clear cell sarcoma of the kidney (CCSK) is the second most common pediatric renal malignancy and represents approximately 3 to 5% of all renal tumors in children. Several histologic variants of CCSK have been described, and to date, two distinct molecular alterations

have been identified. Approximately 80% of CCSKs harbor B-cell CLL/lymphoma 6 (BCL6)-interacting co-repressor (*BCOR*) gene internal tandem duplication (ITD), and an additional 10% are positive for *YWHAE–NUTM2B/E* fusion. The remaining CCSKs are negative for both *BCOR-ITD* and *YWHAE–NUTM2B/E* fusion—the so-called double-negative subcategory. We hypothesize that CCSK is composed of distinct molecular subgroups and that these subgroups could be distinguished by their unique genomic alterations, epigenetic signatures, and immunophenotype.

A cohort of 30 CSSK was reviewed and stained with selected immunohistochemical stains (BCOR, WT-1, INI-1, YAP-1, Cyclin D-1, EGFR, BCL-6, H3K27me3, and p53). All cases were evaluated by Interphase Fluorescence In Situ Hybridization (iFISH) for *YWHAE–NUTM2B/E* gene rearrangement and via targeted PCR for *BCOR-ITD* and Epidermal growth factor receptor *(EGFR)-ITD. The tumor-specific methylation signature and CNAs were* derived using the Illumina Infinium 850K methylation array. Anaplastic and non-anaplastic Wilms tumors were included among the control samples.

Using unsupervised cluster analysis of the methylation data, the CCSKs cluster into two distinct subgroups. The largest group includes the *BCOR-ITD* positive CCSKs and show a comparatively stable genome. The second distinct cluster contains the *YWHAE* gene-rearranged and double negative tumors. This cluster is characterized by more frequent CNAs and uniformly expresses cytoplasmic WT1. One double-negative CCSK harbored an *EGFR-ITD*.

Conclusions: Our data suggest that CCSK represents two molecularly distinct subgroups, and supports the concept that *BCOR-ITD* and *YWHAE-NUTM2B/E* fusion are mutually exclusive. The *YWHAE–NUTM2B/E* rearranged and double negative cases are closely related, and can be identified by their distinct diffuse cytoplasmic WT1 expression. Whether these subgroups have prognostic significance or demonstrate differences in clinical behavior is yet to be determined.

2001 High expression of pAKT and pmTOR in multicystic renal dysplasia

Herve Sartelet[1], Pierre-Simon Jouk[2], Alexia Apostolou[3], Brice Poreau[2]. [1]CHU de Grenoble, Grenoble, Isere, [2]CHU de Grenoble, [3]CHU de Grenoble, Eybens, Isère

Background: Multicystic renal dysplasia is congenital cystic anomaly of the kidney caused by abnormal metanephric differentiation associate with immature tubules surrounded by mesenchymal collars and islands of immature mesenchyme are present between the cysts. The PI3K-Akt-mTOR signaling pathway is a key regulator of normal cellular processes involved in cell growth, proliferation, motility, survival, and apoptosis. Activation of the PI3K-Akt-mTOR pathway results in the survival and proliferation of tumor cells in many human cancers.

The aim of this study is to analyse the topographic expression of Phospho-AKT and Phospho-mTOR in normal renal development and in multicystic dysplastic kidney.

Design: The samples came from Grenoble University Teaching Hospital legally declared collection of embedded tissue sections collected after autopsy for perinatal and infant death performed for a diagnostic purpose. Written consent was obtained from the parents or guardians at the time of the request for autopsy authorization and for research authorization on normal and abnormal development. 17 cases of normal fetal kidneys of different ages of development used for control and 13 cases of pathological kidneys with MCDK were mainly analyzed by immunohistochemistry in order to evaluate the expression of Phospho-AKT (S473) and Phospho-mTOR.

Results: Phospho-AKT and Phospho-mTOR are early expressed in normal renal development and in identical manner for every structure derived from the ureteric bud such as collecting ducts and urothelium. Later, their expressions differ according to the needs of cell proliferation and differentiation over time by becoming more selective.

In multicystic renal dysplasia, Phospho-AKT and Phospho-mTOR were constantly present with high cytoplasmic expression in cystic epithelium, loose mesenchyme. In primitive tubes, a high expression of both proteins was found in epthelial cells but not in adjacent mesenchyma.

Conclusions: This study demontrated the essential and specific role of PI3K-Akt-mTOR pathway, in the formation of cysts in Multicystic renal dysplasia. Specific inhibitors of these proteins could be a good way to treat some less severe forms of renal cystic diseases in postnatal.

2002 Clinical Application of Whole-Genome Arrays in Diagnostic Studies of Pediatric Solid Tumors

Lina Shao[1], Amer Heider[1], Carl Koschmann[1], Sandra Camelo-Piragua[1], Raja Rabah[1]. [1]University of Michigan, Ann Arbor, MI

Background: Recurring cytogenetic abnormalities play important roles in the diagnosis and prognosis of pediatric solid tumors. However, classic cytogenetics is often challenging due to tissue culture failure, treatment effect, or inadequate sampling. Whole-genome array analysis (WGA) overcomes the need of cell culture and only uses small amount of DNA. It was implemented for the detection of cryptic copy number abnormalities and copy-neutral loss of heterozygosity for both hematological malignancies and pediatric solid tumors in our institution.

Design: We retrospectively reviewed diagnostic samples obtained from pediatric solid tumors with cytogenetic tests between March 2015 - August 2017. WGA using Affymetrix CytoScan platform were performed in a total of 157 samples, and conventional cytogenetics was performed in 146 of them. We compared array results with karyotype or FISH results and correlated with histological diagnoses.

Results: A variety of solid tumors were submitted for cytogenetic tests, the most common ones included neuroblastomas (N=21), sarcomas (N=18), Wilms tumors (N=17), teratoma (N=16), and brain tumors (N=15). One hundred and eighteen (75.2%) specimens had at least one copy number aberrations or region of loss of heterozygosity detected by WGA. Genetic abnormalities that were associated with diagnosis, prognosis or therapy were observed in 99 of them (63.1%). Genetic results indicative of a malignant process were observed in 3 cases of benign lesion; genetic results not consistent with original histological diagnosis were noted in an Ewing sarcoma and two brain tumors. Conventional cytogenetics was performed in 146 samples, 58 of them (39.7%) had an abnormal karyotype or abnormal FISH results, and the remaining had a normal karyotype (22.6%) or inadequate cells for cytogenetic analysis (37.7%). Abnormal array results were detected in 91.3% of the samples with an abnormal karyotype, in 39% of the samples with a normal karyotype, and in 76.4% of the samples with an inadequate cytogenetic analysis.

Conclusions: WGA improved detection of cytogenetic abnormality rate from 39.7% to 75.2%. It provided clinically relevant results in over 60% of the tumors, and improved diagnosis, prognosis and treatment of pediatric solid tumors. We suggest that WGA be considered as the first tier cytogenetic test in most pediatric solid tumors, especially when material is limited, with the exception when balanced rearrangements are the common recurring abnormalities.

2003 Examination of SSTR2A and CXCR4 Expression in Pediatric Neuroblastic Tumors and Wilms Tumor

Devin Shrock[1], Daniel Pelletier[2], M. Sue O'Dorisio[3], Andrew Bellizzi[1]. [1]University of Iowa Hospitals and Clinics, Iowa City, IA, [2]University of Iowa Hospitals and Clinics, Coralville, IA, [3]University of Iowa Hospitals and Clinics

Background: Meta-iodobenzylguanidine (MIBG), a norepinephrine analogue, is concentrated in cells of the autonomic nervous system and cognate tumors. MIBG-based nuclear medicine imaging is routinely utilized to stage neuroblastoma (NB) patients at initial clinical presentation, and patients with primary resistant or recurrent disease may be treated with MIBG-based radionuclide therapy. The G protein-coupled receptor SSTR2A is highly expressed by neuroendocrine tissues and tumors, and the chemokine receptor CXCR4 is highly expressed by poorly differentiated neuroendocrine carcinomas. SSTR2A and CXCR4-based imaging and radionuclide therapy are being pursued in adult neuroendocrine tumors.

Design: Immunohistochemistry for SSTR2A and CXCR4 was performed on tissue microarrays (tumors arrayed as triplicate 1 mm cores) of 68 neuroblastic tumors (NBTs; 6 undifferentiated [U], 35 poorly differentiated [PD], 10 differentiating neuroblastomas [D]; 11 ganglioneuroblastomas [GNB]; 6 maturing ganglioneuromas [MG]) and 39 Wilms tumors. Expression was evaluated for intensity (0-3+) and extent (0-100%) with an H-score calculated (intensity*extent). Fisher's exact test was used with $p < 0.05$ considered significant.

Results: SSTR2A was expressed by 49% of NBTs and 21% of Wilms tumors, though very weakly so in the latter. CXCR4 was expressed by 22% of NBTs and 45% of Wilms tumors. Detailed expression data are presented in the Table.

Table: SSTR2A and CXCR4 Expression in Neuroblastic Tumors and Wilms Tumor

	SSTR2A				CXCR4			
	% positive	p	Mean (Median) H-score (if positive)	p	% positive	p	Mean (Median) H-score (if positive)	p
NBT	49%	.0039	38 (13)	0.047	22%	0.026	54 (33)	0.84
Wilms	21%		5 (5)		45%		40 (35)	

Degree of differentiation did not appear to influence the frequency of SSTR2A expression (44% in U/PD vs. 58% in D/GNB/MG; p=0.32), but CXCR4-positivity was largely restricted to more primitive tumors (32% U/PD vs. 8% of D/GNB/MG; p=0.034).

Conclusions: SSTR2A is expressed by half of NBTs regardless of differentiation, representing a potential therapeutic target in advanced disease. CXCR4 is preferentially expressed in more primitive NBTs, in which it again represents a potential therapeutic target. Of note, nearly half of Wilms tumors expressed CXCR4 (at similar levels as in NBTs) with potential diagnostic and therapeutic implications.
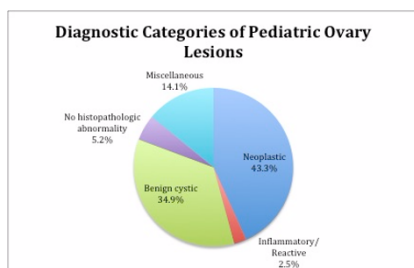
2004 Spectrum of Pediatric Ovary Pathology: The Dallas Experience

Amanda Strickland[1], *Charles Timmons*[2], *Dinesh Rakheja*[3]. [1]University of Texas Southwestern, Dallas, TX, [2]Children's Medical Center, Dallas, TX, [3]University of Texas Southwestern Medical Center, Dallas, TX

Background: Pediatric ovarian diseases encompass a wide range of pathologic processes, which differ significantly in behavior and prognosis. For example, while malignant ovarian tumors may be life threatening, both malignant and benign ovarian tumors may cause significant morbidity, such as potential infertility. Thus, prompt and accurate diagnosis is essential for appropriate management. The purpose of this study is to describe the spectrum and incidence of ovarian pathology at our institution over the past 20 years.

Design: After approval by the Institutional Review Board, a review of all pathology reports from a large metropolitan pediatric hospital, from January 1, 1996 to April 1, 2017 was conducted. Inclusion criteria were specimens containing ovarian tissue from female patients ranging from birth to age 21 years. Any cases from intersex patients were excluded.

Results: Cases were retrieved for 595 female patients with 729 specimens. The age ranged from 1 day to 19 years (mean 11.8 years, median 13 years). As shown in the pie chart [FIGURE 1], neoplasms comprised the majority of the diagnoses. The most common benign neoplasm was mature teratoma (n=174, 24.4% of all cases) followed by serous cystadenoma (n=42, 5.9%). The most common malignant neoplasm was malignant mixed germ cell tumor (n=14, 2%), followed by juvenile granulosa cell tumor and Sertoli-Leydig cell tumor (each n=8, 1.1%). Metastatic neoplasms included 1 case of anaplastic Wilms tumor and 2 cases of lymphoblastic leukemia/lymphoma. The most common benign cyst was follicular cyst/ cystic follicle (n=98, 13.7%), followed by corpus luteum cyst (n=74, 10.4%) and paratubal cyst (n=28, 3.9%). Inflammation and/or reactive changes were seen in 18 cases (2.5%). Torsion (or consistent with torsion) was the most common diagnosis (n=88, 12.3%) in the miscellaneous category. Interestingly, 37 specimens (5.2%) demonstrated no significant histopathologic abnormality.

Diagnostic Categories of Pediatric Ovary Lesions

- Miscellaneous 14.1%
- No histopathologic abnormality 5.2%
- Benign cystic 34.9%
- Neoplastic 43.3%
- Inflammatory/ Reactive 2.5%

Conclusions: This is one of the largest clinico-pathologic studies of pediatric ovarian lesions. Ovarian lesions are not uncommon in children and require special attention due to the relatively wide differential diagnoses and the potential significant consequences later in adulthood. Similar studies from other pediatric institutions from around the world may illustrate any geographic or ethnic variations in pediatric ovarian pathology.

2005 Clinical Impact of the New WHO 2016 Brain Tumor Classification for Pediatric Glial Tumors

Mariona Suñol[1], *Andres Morales*[2], *Carmen de Torres*[2], *Vicente Santa-Maria*[2], *Iban Aldecoa*[3], *Ofelia Cruz*[4], *Jaume Mora*[2], *Teresa Ribalta*[5]. [1]Hospital Sant Joan de Deu, Barcelona, [2]Hospital Sant Joan de Deu, [3]Hospital Clinic of Barcelona, Spain, , [4]Sant Joan de Deu, [5]Hospital Sant Joan de Déu, Esplugues de Llobregat, Barcelona

Background: Glial tumors are the most frequent CNS tumors in childhood. Historically, tumor classification has relied upon histology and immunohistochemistry. Recently, molecular alterations have improved the ability for glial tumors classification and prognostication. The 2016 WHO CNS tumor classification incorporated molecular parameters modifying some of the glial categories. It is to be determined whether or not this revision provides more accurate risk-group classification, prognostication, and its impact in therapy.

Design: We assessed 192 tumors. Initial diagnosis was done according to the 2000 and 2007 WHO classifications. All cases were histologically re-evaluated. Additionally, immunohistochemical, cytogenetic and molecular analysis were performed following the WHO 2016 classification recommendations. Our main objective was to identify the potential impact of the new classification in our retrospective cohort in terms of risk-group classification, prognosis and therapeutic approach.

Results: The initial diagnosis according to the previous editions of the WHO classification included: low-grade glioma (LGG) 121; high-grade glioma (HGG) 30; glioneuronal tumor (GNT) 28; diffuse midline glioma (DIPG) 2; gliomatosis cerebri (GC) 2; high-grade neuroepithelial tumor (HGNET) 7; insufficient material 2. Following reassessment using the new WHO 2016 criteria, the tumors were regrouped as follow: LGG 112; HGG 12; GNT 32; DIPG 0; GC 0; HGNET 5; HGG-H3K27M-mutant 19; HGG-H3G34R: 2; insufficient material 10. Most tumors remained in the same category. However, 46 (30%) changed histological grade. The majority of cases were reclassified from LGG to pilocytic astrocytoma and HGG to astrocytoma grade IV according to molecular results. One tumor initially diagnosed as grade II, was re-classified as a diffuse midline glioma H3K27M-mutated and in 2 cases previously diagnosed as grade III, the KIAA1549-BRAF presence reclassified them as pilocytic astrocytomas.

- The most relevant molecular alterations that allowed to reclassify pediatric gliomas are the BRAF fusion and the K27M mutation.

- Risk-group classification, prognostication and therapy would have been different at diagnosis in 3 cases.

- Even though the 2016 WHO CNS tumor classification system allowed a more accurate diagnosis and prognostication in a third of cases, in only 3/172 patients there would have been a major impact in prognosis and therapy at diagnosis.

2006 PD-L1 Expression in Pediatric Soft Tissue Tumors: Angiomatoid Fibrous Histiocytoma and Inflammatory Myofibroblastic Tumor

Brandon Umphress[1], *Demirkan Gursel*[1], *Jian-Jun Wei*[1], *Pauline Chou*[2]. [1]Northwestern University, Chicago, IL, [2]Lurie Children's Hospital of Chicago, Chicago, IL
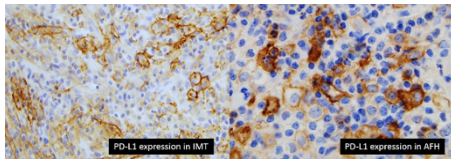
Background: Angiomatoid fibrous histiocytoma (AFH) and inflammatory myofibroblastic tumor (IMT) are classified as intermediate, rarely metastasizing tumors and commonly recurring entities in the WHO classification of soft tissue tumors. These are commonly seen in the pediatric population yet treatment options are limited. Both are characterized by a distinct inflammatory component suggesting that immune checkpoint pathways including programmed death signaling (PD-1/PD-L1) may play a role in these entities. Additionally, PD-L1 expression by immunohistochemistry (IHC) of high-grade sarcomas has been associated with a poorer prognosis and overall survival. Our objective was to characterize PD-L1 expression in pediatric AFH and IMT, as this has not been done to date.

Design: 5 cases from 5 patients with AFH and 9 cases from 7 patients with IMT (total of 14 cases, 12 patients, mean age = 11.2, range 1-17 years) from 1998-2017 were evaluated. Diagnoses of AFH and IMT from whole tissue sections were confirmed by two pathologists. ALK IHC (Leica Biosystems, clone 5A4) was performed on all IMTs. PD-L1 IHC (Cell Signaling, E1L3N on IMT & Ventana, clone SP142 on AFH) was performed on all cases. PDL-1 expression on tumor cells only was scored on a semi-quantitative scale of 0-6 by evaluating extent of membranous expression (0=negative, 1=weak, partial, 2=intermediate, 3=strong, diffuse) and percentage of tumor cell positivity (0=negative, 1=<1% positivity, 2 = ≥ 1-4%, 3 = ≥ 5%). Scoring was independently performed by two pathologists. Frequency of PDL-1 expression was determined. Simple student t-test was used to compare PDL-1 expression in AFH and IMT. Association of ALK and PDL-1 positivity using the fisher's exact test was performed using Simple Interactive Statistical Analysis (SISA).

Results: 7 of 9 cases (78%) of IMT and 4 of 5 cases (80%) of AFH demonstrated PD-L1 expression. ALK was observed in seven of nine (78%) IMT cases. Mean PD-L1 score for IMT was 3.89/6 while AFH was 3.93/6. PD-L1 expression between IMT and AFH exhibited no difference (p = 0.521). ALK and PD-L1 expression were not associated (p = 0.417) and 1/2 of ALK-negative cases expressed PD-L1.

Inflammatory Myofibroblastic Tumors	PD-1 %	Membrane Expression	Tumor % Positivity	Total PD-1 Score (0-6)	ALK
Abdominal mass, 42 cm	20-25%	3	3	6	Positive
Small bowel mass, 7.5 cm	1-4%	3	2	5	Positive
Bladder biopsy	10-15%	3	3	6	Positive
Bladder mass, 8 cm	5-10%	2	3	5	Positive
Pelvic mass, 6 cm	Negative	0	0	0	Positive
Lung mass, 2.3 cm	1%	1	2	3	Positive
Lung mass, 6.5 cm	25-30%	3	3	6	Negative
Anterior mediastinum, 2.0 cm	Negative	0	0	0	Negative
Left vocal cord, 0.4cm	1%	2	2	4	Positive
Angiomatoid Fibrous Histiocytoma	**PD-1 %**	**Membrane Expression**	**Tumor % Positivity**	**Total PD-1 Score (0-6)**	
Multiple inguinal masses, 1.2-3.7 cm	10-15%	3	3	6	
Left posterior upper extremity mass, 3.1 cm	1%	1	2	3	
Left perifibular mass, 7 cm	5-10%	3	3	6	
Skin, no gross mass	Negative	0	0	0	
Scalp, cystic lesion, 1.5 cm	5-10%	2	3	5	

PD-L1 expression in IMT   PD-L1 expression in AFH

Conclusions: Our findings suggest that PD-L1 is expressed in the majority of pediatric AFH and IMT. Subsets of these soft tissue tumors, especially those not amenable to traditional treatment modalities, may be future candidates for PDL-1 immunotherapy. Future studies in larger cohorts are needed for further validation.

2007 Is Lymphocytic Esophagitis in Children a Prelude for Eosinophilic Esophagitis?

Debbie Walley[1], Tejal Patel[2], Anas Bernieh[1], Ali Saad[1]. [1]University of Mississippi Medical Center, Jackson, MS, [2]University of Mississippi Medical Center, Madison, MS

Background: Lymphocytic esophagitis (LyE) in children remains poorly understood. Here we report 7 patients diagnosed initially with LyE and, upon follow-up, developed eosinophilic esophagitis (EoE).

Design: All esophageal biopsies performed on children (≤18 years-old) in the last 10 years were reviewed. Cases with ≥20 lymphocytes/high-power field and rare eosinophils (≤2) are included. Demographics, clinical and histological findings were retrieved from pathology reports and medical records in accordance with the institutional research board guidelines. Lymphocytic count was generated by counting the numbers of lymphocytes at 40X in a single hot spot.

Results: The search resulted in 24 patients (age range: 1-17.5 years; mean: 6.9 years). They consisted of 11 males (age range: 1-17.5; mean: 6.9 years) and 13 females (age range: 2-16.5 years; mean: 6.9 years). The most common presentation was dysphagia (33.3%) followed by reflux (29.2%), abdominal pain (29.2%), and nausea and vomiting (8.3%). Esophageal endoscopic findings ranged from normal to erosive esophagitis. Ileal and colonic endoscopy ranged from normal to severe active inflammation.

The mean number of lymphocytes was 40.4 (range 21-71 lymphocytes). There was correlation between the number of lymphocytes and a particular final diagnosis. In addition, there was no difference in the number of lymphocytes between males and females.

Follow-up showed that 7 patients were diagnosed with gastroesophageal reflux disorder, 7 patients with eosinophilic esophagitis, 3 patients with Crohn's disease, 1 patient with celiac disease, 1 patient with ulcerative colitis, and 3 patients with gastritis. Follow-up in 3 patients did not disclose any particular entity and were labeled as having LyE. EoE developed a mean of 17 months (range 13-21 months) after the first endoscopy that showed LyE. This finding highlights the importance of regular endoscopic and histologic follow-up of patients with LyE.

Conclusions: In this series, the largest in the pediatric population, 7 patients (29.2%) developed EoE upon follow-up. Our series suggests that LyE might not be a disease by itself but rather an early histologic feature of several entities, particularly EoE. Regular follow-up with histological examination of these patients is necessary in order to unmask the final diagnosis. In this study, EoE developed as early as 13 months after the initial endoscopy and, therefore, follow-up at 6 months interval is probably justified.

2008 Neuroblastoma PTPome Analysis Unveils Association of PTPN1 And DUSP5 Expression With Poor Prognosis

Laura Zaldumbide[1], Olaia Aurtenetxe[2], Asier Erramuzpe[2], Mónica Saiz[3], Ricardo López-Almaraz[4], Verónica Caamaño[3], Jesús M Cortés[5], Ena Fernández-Lomana Idiondo[6], Aitziber Marcos Muñoz, Caroline E Nunes-Xavier[7], Jose I López[3], Rafael Pulido[8]. [1]Cruces University Hospital, Barakaldo, Vizcaya, [2]Biocruces Health Research Institute, [3]Cruces University Hospital, [4]Cruces University Hospital, Barakaldo, Bizkaia, [5]Basque Foundation for Science, [6]Hospital Universitario de Cruces, Barakaldo, Bizkaia, [7]Institute of Cancer Research, [8]Biocruces Health Research Institute, Barakaldo, Bizkaia

Background: Differentiation of neuroblastoma (NB) cells is the rational of some maintenance therapies for high-risk NB. Protein tyrosine phosphatases (PTPs) regulate neuronal differentiation and survival, but their expression patterns in NB are scarcely known. The aim of this study was to identify PTPs that might represent new biomarkers or potential regulators of NB cell growth.

Design: A comprehensive expression analysis of the extended PTP superfamily was performed on tissue microarrays or histological sections of 44 human NB tumor samples, including 16 high-risk NB specimens. The immunohistochemical analysis included a panel of 12 anti-PTP antibodies.

Results: High-risk NB human samples displayed a significant enrichment in high expression of DUSP5. PTPN1 and DUSP5 were highly expressed in most of the metastatic NB when compared with the non-metastatic samples. PTPN1 and DUSP5 displayed low or no expression in most of the tumors showing a total regression. These findings suggest a potential involvement of PTPN1 and DUSP5 in malignant NB progression, and argue for PTPN1 and DUSP5 high expression as potential surrogate markers defining poor prognosis in NB.

Clinic-pathologic characteristics of study population		
Patients (n=44)		
	n	%
Gender		
Male	21	48
Female	23	52
Age at diagnosis (months)		
<18	29	66
>18	15	34
Risk		
Low	19	43
Medium	9	20
High	16	36
Stage		
Metastatic	11	25
Non-metastatic	33	75
MYCN		
Amplified	8	18
Non-amplified	25	57
Regresssion		
No	27	61
Partial	2	4.5
Total	15	34
Dead	10	23

Conclusions: We identified PTPs that could modulate differentiation and growth of NB cells and found an association between PTPN1 and DUSP5 high expression NB and poor prognosis. PTPN1 expression correlates with metastasis and poor prognosis in several human cancers, whereas a tumor suppressor role for DUSP5 has been proposed. Our results provide insights into the dynamic expression and potential involvement of PTPs in NB, and identify novel candidate NB prognostic biomarkers, which need to be validated in further work. This may have important clinical implications for a better patient stratification and for the implementation of future novel targeted therapies.

2009 Independent evaluation of the new international risk stratification system for hepatoblastoma using a single institution cohort

Shengmei Zhou[1], Larry Wang[2], Leo Mascarenhas[2]. [1]Los Angeles, CA, [2]Children's Hospital of Los Angeles, Los Angeles, CA

Background: The Children's Hepatic tumors International Collaboration (CHIC) group recently developed a new international risk stratification system for hepatoblastoma. Its risk stratification trees include PRETEXT stage, metastases, alpha-fetoprotein level, PRETEXT annotation factors, age, and tumour resectability and categorize patients into four risk groups: very low, low, intermediate, and high. However, its ability to predict overall survival has not been evaluated in an independent group of patients.

Design: We analyzed the retrospectively collected data of 99 consecutive hepatoblastoma patients (63 males, age ranges from 5 months to 18 years) who were treated at our institution between 2000 and 2016. Using the risk stratification trees, each patient was assigned to a risk group.

Results: There were 17, 31, 22 and 29 patients in very low, low, intermediate, and high risk groups, respectively. After a median follow-up of 3.1 years, there were 14 total cancer specific deaths. Estimated 5-year overall survival rates by the CHIC risk classification trees were 100%, 91.4%, 94.4 %, and 60% in patients in very low, low, intermediate, and high risk groups, respectively. There is no statistical significance among very low, low and intermediate risk groups. The Hazard Ratio (HR) of death of patients in high risk group was 2.86 (95% CI 1.28 to 6.37, p <0.01) compared to other groups. Twenty-eight patients accepted liver transplantation after chemotherapy, mainly in intermediated risk group (n=14) and high risk group (n=9). None of patients in very low risk group needed liver transplantation.

Overall survival (%) vs Years after first diagnosis. Very low risk, Intermediate risk, Low risk, High risk.
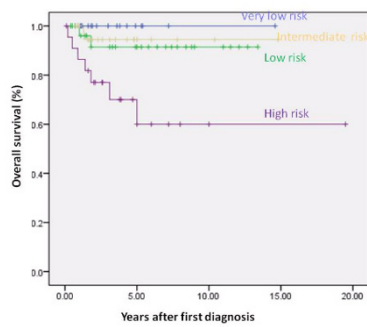
Conclusions: Our data suggest that the new international risk stratification system predicts the overall survival well in very low and high risk groups. However, it performs poorly in low and intermediate risk groups. The status of liver transplantation may be incorporated in risk stratification trees.

2010 Omphalocele Related Genetic Abnormalities

Huifang Zhou[1], Christopher J O'Conor[2], Louis P Dehner[1]. [1]Washington University School of Medicine, St Louis, MO, [2]Washington University, St. Louis, MO

Background: Omphaloceles, a type of congenital abdominal wall defect, are frequently associated with chromosomal aneuploidies. It has been previously shown that omphaloceles associated with genetic abnormalities have a worse prognosis than isolated omphaloceles. Single gene knockdown can cause abdominal wall development defect in animal model. However, there is no omphalocele-related gene reported in human being. High resolution chromosomal microarray analysis (CMA) can detect segmental alterations less than 5 Mb, which enables the identification of omphalocele-related genes.

Design: To identify omphalocele-related genes, a CoPath database search (1/2009 - 7/2017) was performed using key words "omphalocele" and "CMA". The results were reviewed and 32 cases were confirmed with established clinical diagnosis of omphalocele and valid CMA results. All CMAs were performed in the same laboratory with a standardized protocol and reporting criteria. Copy number gains/losses and corresponding genes were assessed by the Affymetrix CytoScan HD array and analyzed by the Affymetrix Chromosome Analysis Suite.

Results: Of the 32 cases, five (5/32, 16%) have segmental gains/losses, involving 22 genes. The results are summarized in Table 1. Interestingly, Giancarlo Ghiselli and Steven A Farber have reported that GLCE knockdown impairs abdominal wall closure in zebrafish. We also identified GLCE gene alteration in our case 5. These data highlight the importance of GLCE in abdominal wall development. Further study of the function of GLCE and other genes might lead to a better understainding of the molecular mechanism of omphalocele.

Table 1

Case	Congenital Anomalies	Segmental Gains/Losses	Involved Genes
1	Omphalocele, ileal atresia, dysmorphisms	Gain (1p36.32) 818 Kb	ACTRT2, PRDM16, ARHGEF16, MEGF6
2	Omphalocele, syndactyly, posterior cleft palate	Loss (3q11.2) 157 Kb	EPHA6 (intron)
3	Giant omphalocele	Gain (7p22.2) 865 Kb	CARD11, SDK1, RPL21P72, RN7SKP130
4	Omphalocele, bladder exstrophy, complex congenital heart disease	Gain (13q33.3 q34) 20 Mb	IRS2, COL4A1, COL4A2, CARS2, ING1
5	Giant omphalocele, pulmonary hypoplasia, spinal curvature	Gain (15q23) 676 Kb	NOX5, EWSAT1, GLCE, PAQR5, KIF23, RPLP1, DRAIC, PCAT29

Conclusions: To date, this is the first study of genetic abnormalities in infants with omphalocele. These findings provide an important step in better understanding the pathogenesis and prognosis of omphalocele. The genes found in our case series appear to vary among the infants analyzed, though there could be shared functional changes downstream of these genetic alterations. We believe that future implementation of RNA sequencing and analysis of their proteomic expression may lead to a better understanding of the genotype-phenotype relationship of omphalocele.

Key words: omphalocele, abdominal wall defect, segmental chromosomal gains/losses, genetic abnormalities, GLCE

FIG. 1991

Case No.	Inherited Bone Marrow Failure Syndrome	Age of Diagnosis, Sex	Presentation	Blasts %	Cytogenetics	FISH	Pathogenic gene	Follow-up
1	Fanconi anemia	8 years, M	Pancytopenia, fever, anorexia	10-15%	Del(1p), t(3;6), del(7p), del(7q), -22	N/A	Biallelic mutations in FANCA	Alive, 3 years
2	Thrombocytopenia absent radii syndrome	11 years, F	Pancytopenia, fever	10-15%	46,XX	Negative for PML/RARa, AML1/ETO, CBFB, MLL, loss of chromosome 5 and 7	600 base pair microdeletion at chr.1q21.1, including RBM8A gene	Alive, 11 years
3	Shwachman-Diamond syndrome	18 years, M	Fatigue, weight loss	15-20%	46,XY	N/A	SDS (c.183_184det-TAinsCT(K62X); SDS c.258+2T>C (IVS +2T>C)	Alive, 1 month